Cell. Mol. Life Sci. 63 (2006) 2377–2386
1420-682X/06/202377-10
DOI 10.1007/s00018-006-6264-7

Cellular and Molecular Life Sciences

Research Article

Characterization of apoptosis induced by marine natural products in non small cell lung cancer A549 cells

A. Catassi [a, b], A. Cesario [c, d], D. Arzani [e], P. Menichini [f], A. Alama [a], C. Bruzzo [a], A. Imperatori [b], N. Rotolo [b], P. Granone [c] and P. Russo [a, *]

[a] Translational Research B (Lung Cancer), Department of Integrated Medical Oncology (DOMI), National Cancer Research Institute, Largo Rosanna Benzi 10, 16132 Genoa (Italy), Fax: +39 0105600217, e-mail: patrizia.russo@istge.it
[b] Center of Thoracic Surgery, University of Insubria, Varese (Italy)
[c] Department of Surgical Science, Division of General Thoracic Surgery, Catholic University, Rome (Italy)
[d] Clinical Respiratory and Pathology Translational Laboratory, IRCCS San Raffaele, Rome (Italy)
[e] Division of Hygiene, Catholic University, Rome (Italy)
[f] Department of Translational Oncology, Molecular Mutagenesis Unit, National Cancer Research Institute, Genoa (Italy)

Received 7 June 2006; received after revision 13 July 2006; accepted 9 August 2006
Online First 28 September 2006

Abstract. The effects of different marine derived agents were studied in A549 cell growth. These drugs induced cell cycle arrest at the G_2-M phase associated with the up-regulation of GADD45α–γ and down-regulation of c-Myc. In treated cells, GADD45α–γ and c-Myc were up- and down-regulated, respectively. A cascade of events leading to apoptotic mitochondrial 'intrinsic' pathway was observed in treated cells: (1) dephosphorylation of BAD serine[136]; (2) BAD dissociation from 14-3-3 followed by its association with BCL-XL; (3) cytochrome *c* release; (4) caspase-3 activation, and (5) cleavage of vimentin. Caspase(s) inhibitor prevented the formation of cleavage products and, in turn, apoptosis was inhibited through a p53-independent mechanism. Moreover, these compounds did not activate NF-κB. Our findings may offer new insights into the mechanisms of action of these agents in A549 cells. The better understanding of their effects might be important to fully exploit the potential of these new drugs.

Keywords. Marine agents, apoptosis, BAD, c-myc, GADD45, non small cell lung cancer.

Introduction

Small molecules derived from plant and microbial sources have long had a significant role in cancer therapy. As a class, they have the advantage of having greater chemical diversity than typical synthetic chemical libraries. Thus, looking back at the history of cancer therapies, natural products have always played a major role in medical oncology. Almost 60% of drugs approved for cancer treatment are of natural origin: vincristine (VCR), irinotecan, etoposide, taxanes and camptothecines are all examples of plant-derived compounds. Furthermore, dactinomicine, anthracyclines, mitomycin and bleomycin are anticancer agents derived from microbial sources [1–4]. Until the mid-1960s, investigation of natural products from marine organisms was essentially non-existent. Since then, ~10 000 new structures have been isolated from marine microorganisms, seaweeds, sponges, soft corals, and marine invertebrates, such as bryozoans, echinoderms, molluscs and ascidians. The best example of a new class of antitumor

* Corresponding author.

drugs from a marine source is Ecteinascidin 743 (ET-743; *Yondelis; Trabectedin*) isolated from the Caribbean marine tunicate *Ecteinascidia turbinata*. ET-743 targets DNA by binding in the minor groove in GC-rich sequences and alkylating the 2-amino group of guanine. Recently, ET-743 demonstrates clinical activity as first-line therapy against soft tissues sarcomas with acceptable toxicity [5].

Molecular-targeted drug discovery and its application to marine natural products are continuously evolving disciplines. Apoptosis represents an universal and efficient form of cell death that is executed through a highly ordered intrinsic cellular suicide program. A number of marine natural products that induce apoptosis were first identified as cytotoxic agents, and their apoptotic activity was discovered later in secondary pharmacological evaluations in tumor cell lines [6]. Among these we selected six different marine natural products that modify the cellular cytoskeleton acting on tubulin [6] and we characterized their apoptotic potential in the human non small cell lung cancer (NSCLC) cell line A549.

In the early 1970s, Pettit and colleagues [7] discovered the extremely potent anticancer properties of some extracts from the sea hare *Dolabella auricularia,* named Dolastatins. The low concentration of the active principle (DLS10) in sea hares implicated a cyanobacterial diet as its origin, and this was subsequently confirmed by direct isolation of DLS10 from the marine cyanobacterium *Symploca*. DLS10 is a pentapeptide that strongly affects microtubule assembly and tubulin-dependent guanosine trisphosphate hydrolysis, causing cell cycle arrest in metaphase. Auristatin-PE (*Soblidotin*, TZT-1027) is a derivative of DLS10 with superior preclinical activity. DLS15, also derived from a cyanobacterium, showed a much weaker binding to tubulin compared with DLS10 [8, 9]. The complexity, the low yield of DLS15 chemical synthesis and its poor water solubility prompted the development of different synthetic analogues compounds, like the LU103793 (*Cematodin*). Spongistatins and halichondrins are polyether macrolides of marine origin. Spongistatin 1, a macrocyclic lactone polyether from the marine sponge *Hyrtios erecta*, is a noncompetitive inhibitor of the binding of vinblastine and DLS10 to tubulin, causing inhibition of microtubule assembly and cell death. Halichondrin B was isolated by various unrelated sponges such as Aninella species. *In vitro*, Halichondrin B non-competitively inhibits the binding of vinblastine to tubulin, indicating that it may bind to tubulin in the *Vinca* binding domain and prevent the polymerization of tubulin into microtubules [10]. When compared with other microtubule-targeted classes of drugs, the halichondrins exhibit a unique constellation of effects on the conformation of tubulin, as indicated by their consequences on tubulin alkylation, on the chemical cross-linking of tubulin, and on the binding to tubulin of the hydrophobic probe, bis-8-anilinonaphthalene sulfate [10]. These data have led to the idea that the halichondrins interact with tubulin in a manner distinct from that of other microtubule-targeted drugs and, thus, they might possess unique antitumor activities [10]. Because of their biological activity in killing cancer cells (data generated in the NCI drug evaluation program), drugs were generated by chemical synthesis that led to the discovery of one possible clinical candidate E7389 [10]. Curacin A is another potent cancer cell toxin obtained from strains of the tropical marine cyanobacterium *Lyngbya majuscula* found in Curacao. Its structure is unique in that it contains the sequential positioning of a thiazoline and cyclopropyl ring, and it exerts its potent cell toxicity through interaction with the colchicine drug binding site on microtubules [11–13].

Although characterized by distinct structural differences [14], some of these drugs have shown the tendency to trigger apoptosis [15–18]. In the apoptotic pathway, the Bcl-2 family proteins are well-characterized regulators, consisting of anti-apoptotic and pro-apoptotic members [19, 20]. Pro-apoptotic proteins, such as Bad, act as a gateway for a variety of apoptotic signals. Bad is normally localized in the cytoplasm in an inactive form. Serine phosphorylation of Bad leads to its association with 14-3-3 and, consequently, the inhibition of Bad-induced cell death [21].

In the present study, we further characterize the mechanisms of induction of apoptosis studying the phosphorylation of BAD and its interaction with 14-3-3 or BCL-XL, the cytochrome *c* release from the mitochondria, the activation and the role of caspase-3, the cleavage of vimentin (caspase-3 substrate) and the possible activation of NF-κB. We also characterized the mechanism of the G_2-M arrest, induced by these drugs, looking at the regulation of GADD45 family and c-Myc proteins.

Materials and methods

Cell culture and drugs. Human NSCLC cell line A549 (lung carcinoma) was obtained by our Institutional Cell Repository (Genoa, Italy). Cells were grown in RPMI 1640 (Gibco BRL, Grand Island, NY) supplemented with 10% non-heat inactivated fetal bovine serum (Gibco BRL, Grand Island, NY). Cell counts were determined using a Coulter Counter with Channelyzer attachment to monitor cell size (Coulter Electronics, Hialeah, FL). Cell membranes integrity was determined by trypan blue dye exclusion assay.

Drugs were kindly provided by Dr. G.R. Pettit (Cancer Research Institute, Arizona State University). LU103793 was obtained from KNOLL-BASF (Ludwigshafen, Germany). z-DEVD-fmk was obtained from Calbiochem (EMD Biosciences, Inc. Germany).

Cell proliferation assay. All of the experiments were performed at least three times with a minimum of six

replicates per data point per experiment. A549 cells were plated with an 8-channel pipette at 250 cells/well in 96-well plates Drugs were added 24 h after cell plating and cells treated for 24 h in a final volume of 200 µl. Following treatment, medium was withdrawn and cells were incubated for additional 24 and 48 h in drug-free medium. The MTT-based-assay [3-(4,5-dimethylthiazol-2-yl)-2, 5-diphenyltetrazolium bromide], was used to measure cell growth as described [22]. Value of 50% inhibitory concentration (IC_{50}) was calculated as the drug concentration that inhibits cell growth to 50% of the control sample. IC_{50} values were estimated fitting the data with a non linear regression to the dose-effect model derived by Chou and Talalay [23, 24]: $f_a/f_u = (D/D_m)^m$, where D is the dose of the drug, D_m is the IC_{50}, f_a is the fraction affected by the dose, f_u is the fraction unaffected, and m is a coefficient that determines the sigmoidicity of the curve.

Detection of apoptosis. Apoptosis was detected by DNA secondary fragmentation assay and by internucleosomal DNA fragmentation. In the DNA secondary fragmentation assay, apoptosis associated DNA fragmentation was analyzed by filter binding assay (FBA) as described previously [25]. The FBA was performed under non-deproteinizing conditions using protein-adsorbing filters (vinyl/acrylic copolymers filters, Metricel membrane, 0.8-mm pore size, 25-mm diameter; Gelman; Sciences) according to Bertrand et al. [25]. Results were expressed as the percentage of fragmented DNA in treated cells compared with fragmented DNA in control untreated cells (background) using the formula: $[(F - F_0)/(1 - F_0)] \times 100$ where F and F_0 represent DNA fragmentation in treated and control cells, respectively.

Internucleosomal DNA fragmentation was determined as described previously [26]. Briefly, adherent and detached cells were harvested separately, washed, and lysed with 50 mM/l Tris, pH 7.5, 10 mM/l EDTA, 0.5% Triton X-100, and 0.5 mg/ml proteinase K for 2 h at 50 °C. Samples were then extracted twice with phenol/chloroform/isoamyl alcohol and precipitated with ethanol. The pellet was resuspended in Tris-EDTA and 10 µg/ml ribonuclease A and the DNA was separated on a 2% agarose gel.

Preparation of mitochondria-free cytosolic extracts and whole cell extracts. Cytosolic extracts were prepared as described previously [27]. In brief, A549 cells were harvested by gently scraping and were incubated in a buffer containing 220 nM mannitol and 60 mM sucrose on ice for 30 min. Then cells were broken in a Dounce homogenizer by 70 gentle strokes of a type B pestle. The homogenates were centrifuged at 16 000 *g* for 15 min, and the mitochondria-free supernatants were frozen at –70 °C until further analysis. Extracts of the pellets as well as whole cells extracts were obtained by dissolving in lysis buffer, followed by repetitive vortexing and freeze thawing. After centrifugation at 16 000 *g*, the supernatants were stored at –70 °C.

Immunoblotting. Samples were washed twice with PBS, scraped off the plates, and lysed in cell lysis buffer (50 mM Tris-HCl pH 7.5, 150 mM NaCl, 1% Nonidet P-40, 0.5% sodium deoxycholate, and 0.1% sodium dodecyl sulfate) containing the protease inhibitors [100 µg/ml phenylmethylsulfonyl fluoride (PMSF), 1 µg/ml aprotinin, 1 µg/ml leupeptin, 1 µg/ml pepstatin, 50 mM NaF, 2 mM Na_3VO_4]. Whole cell lysates were boiled, and the protein concentration was determined with the Bradford assay (Bio-Rad Laboratories, Hercules, CA). Equal amounts of protein (20–40 µg) were separated by SDS–PAGE under reducing conditions in 4–20% linear gradient polyacrylamide gels (Ready-Gel; Bio-Rad Laboratories). Primary antibodies for Bcl-XL, 14-3-3, caspase 3, activated caspase 3, vimentin, GADD45α, anti-GADD45β, anti-GADD45γ; c-Myc and actin were obtained from Santa Cruz Biotechnology (Santa Cruz, CA). Polyclonal phospho-specific Bad serine^{112} or serine^{136} antibodies were obtained from New England Biolabs (Beverly, MA). Horseradish peroxidase-conjugated goat anti-mouse or donkey anti-goat antibodies were used as secondary antibodies (Santa Cruz Biotechnology). Proteins were visualized with chemiluminescence's luminol reagents (Amersham Biosciences, Piscataway, NJ).

Co-immunoprecipitation experiments. A phosphorylation serine^{112} BAD antibody (New England Biolabs) was cross-linked to protein G-Sepharose beads (Sigma, St. Louis, MO) using 20 mM dimethylpimelimidate. Post-mitochondrial supernatant fractions (14-3-3) or pellet fractions (Bcl-XL) of control and treated cells were incubated with the immobilized BAD antibody overnight at 4 °C on a rocker table. After repeated washing in 0.1 M PBS, proteins bound to BAD were eluted away from the protein G-Sepharose-BAD antibody complex with 100 mM glycine, pH 2.7, and the eluant was neutralized with 1 M Tris, pH 9.0. Eluted samples were then separated by SDS-PAGE, and immunoblotting was used as above to analyze 14-3-3, and Bcl-XL bound to BAD.

Gel mobility shift assay. Nucleic extracts were prepared according to Vikhanskaya et al. [27]. Briefly, 5×10^5 cells were collected, washed in PBS and pelleted. Pellet was resuspended in 400 µl hypotonic buffer (20 mM HEPES pH 7.9, 10 mM KCl, 0.1 mM EDTA, 0.1 mM EGTA, 1 mM DTT, 0.5 mM PMSF). The cells are allowed to swell on ice for 15 min, after which 25 µl 18% solution of Nonidet NF-40 was added, and the tubes were vigorously vortexed for 10 s. The homogenate was centrifuged for 30 s in a microfuge. The nuclear pellet was resuspended in 50 µl ice-cold buffer (20 mM HEPES pH 7.9, 0.4 M NaCl, 1 mM EDTA, 1 mM EGTA, 1 mM DTT, 1 mM

PMSF) and the tubes were vigorously rocked at 4 °C for 15 min. Nucleic extracts were centrifuged for 5 min in a microfuge at 4 °C and supernatant was frozen as aliquots at –70 °C. Of each cell treatment, 1–3 mg was incubated on ice for 30 min in 15 ml buffer containing 10 mM TRIS pH 7.5, 50 mM NaCl, 1 mM EDTA, 1 mM DTT, 3 mg poly(dI-dC), 2 µl pab65 (Santa Cruz Biotechnology, INC), or non-specific antibodies, 1 ng ^{32}P-end labeled oligonucleotide. Part of the enhancer sequence from the HIV LTR region (ENH7 from –115 to –81: GCTTGCTA-CAAGGGACTTTCCGCTGGGGACTTTCC) was added for another 15 min at room temperature. DNA-protein complexes were separated by electrophoresis through 5% native polyacrylamide gel, dried and visualized [27].

RT-PCR analysis. The mRNA from cell lines was isolated utilizing the Quick Prep Micro mRNA purification kit (Pharmacia AB, Uppsala, Sweden) and quantitated spectrophotometrically. About 200 ng of mRNA from each sample were reverse-transcribed using oligo(dT), following the manufacturer's instructions (GeneAMP RNA PCR kit; Perkin-Elmer Life Sciences, Boston, MA). The primers used for c-myc were (5′-TGGTCTTCCCCTACCCTCT-CAAC-3 and 5′-GATCCAGACTCTACCCTCTCAAC-3′) and for GA3PDH (5′-GGTCATCCCTGAGCTGAACG-3′ and 5′-TTCGTTGTCATACCACGAATTG-3′). Thermal cycling was performed as follows: denaturation at 95 °C for 30 s, annealing at 55 °C for 30 s and extension at 72 °C for 90 s. Thirty-five cycles were performed. Primers were used at a final concentration of 10 µM each, with 500 µM dNTPs (Eurogentec, Seraing, Belgium), and 3 mM $MgCl_2$. Five units of Taq DNA polymerase were used per 50-µl reaction. Ten microliter of PCR product were electrophoresed on a 2% agarose gel containing ethidium bromide and visualized by UV illumination.

Densitometry and statistical analysis. Blots were scanned and analyzed by using NIH IMAGE software (Version 1.62, http://rsb.info.nih.gov/nih-image/Default.html). The ratio between immunoreactive proteins and actin was quantified with an electrophoresis Gel Doc 2000 imaging system coupled to Quantity One™ software (Bio-Rad). Background density was subtracted from the densitometric data obtained for each band. At least three to five independent experiments were performed to obtain mean values ± S.E. Statistical analyses [Student's *t*-test (not significant $p > 0.05$)] were performed with PRISM software (Version 3.0a, Graph-Pad, San Diego, CA).

Results

Inhibition of cell growth and cell cycle regulation. The cytotoxic activity of different marine-derived agents: namely DLS10, Auristatin-PE, DLS15, LU103793, Spongistatin-1, Curacin A and Halichondrin B were evaluated in A549 cell line. Cells were exposed to different concentrations of drug for 24 h, followed by additional time in drug-free medium (0, 24, 48 h) prior to the determination of cell survival evaluated by standardized MTT assay. The IC_{50} [nM] values were reached after 72 h (24 h treatment + 48 h in drug free medium) (Table 1). Curacin A, Auristatin PE and LU103 were the most potent drugs, whereas Halichondrin B was the least potent (Table 1). The IC_{50} induced by cis-platin (CDDP), under the same experimental conditions, was 250.0 ± 4.5 nM. Therefore, although within a broad range, marine-derived agents were more potent agents than CDDP, one of the standard drugs for NSCLC treatment.

Table 1. Cytotoxicity of marine-derived agents in A549 cells. Cytotoxicity of marine-derived agents in A549 cells as determined by MTT assay after 24 h exposure to the drug and additional zero (24 h), 24 h (48 h) and 48 h (72 h) incubation in drug free medium.

Compound	IC_{50} [nM] ± SE		
	24 h	48 h	72 h
DLS10	> 1.0	> 1.0	0.97 ± 0.38*
Auristatin-PE	> 1.0	> 1.0	0.58 ± 0.11*
DLS15	> 1.0	> 1.0	0.74 ± 0.25
Lu103793	> 1.0	> 1.0	0.62 ± 0.32*
Spongistatin 1	> 1.0	> 1.0	1.0 ± 0.0*
Curacin A	> 1.0	1.0 ± 0.0*	0.58 ± 0.32*
Halichondrin B	> 100.0	85.2 ± 1.8*	3.2 ± 0.4*

*$p < 0.002$. Each value is representative of a single experiment, which was repeated at least twice.

As reported [10], these drugs are tubulin-interacting agents that cause microtubule depolymerization. Such a mechanism was confirmed in the A549 cell line by looking at the tubulin polymerization and at the cell cycle distribution (G_2-M arrest; data not shown).

Since GADD45 (α, β and γ) plays a role in the G_2/M checkpoint [28], we determined its expression level in logarithmically growing cell cultures (Fig. 1). In these cells, the treatment induced up-regulation of GADD45α and γ, whereas GADD45 β was reduced, indicating that all three members of the GADD45 family are regulated by these marine derived agents in A549 cells (Fig. 1). The c-myc (protein and mRNA) expression was also analyzed, in view of the fact that the c-myc transcription factor represses the GADD45α promoter by a polymerase II recruitment mechanism [29]. We found that c-myc was inhibited both at the mRNA (Fig. 1c) and protein (Fig. 1a) levels, suggesting its involvement in the GADD45 modulation after these marine derivative treatments.

A role of p53 in the regulation of GADD45 and in G_2-M arrest was also investigated. A549 cells endogenously express a wild-type p53 protein [30] that is strongly induced after treatment with CDDP (Fig. 2). After treatment with DLS10, p53 induction was not observed at different times

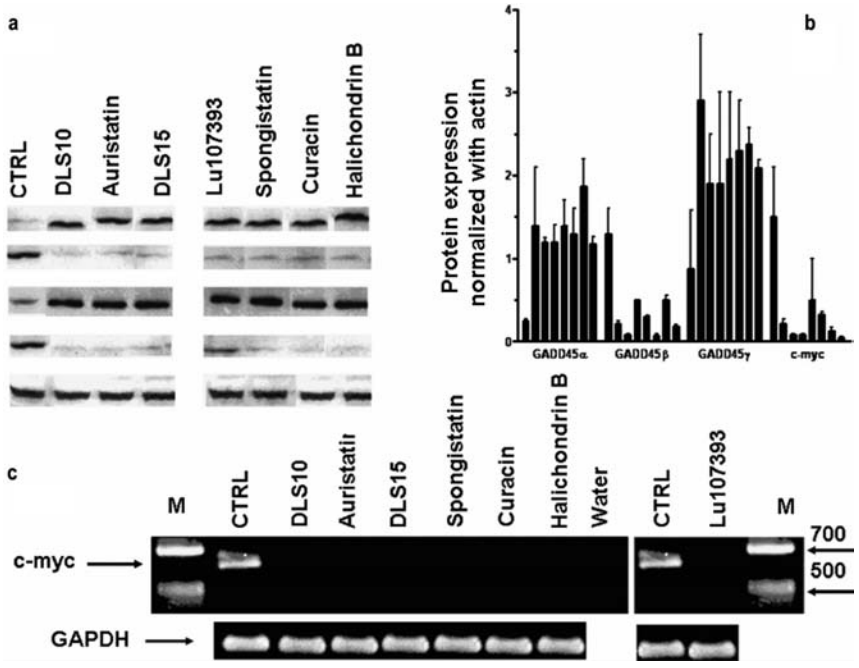

Figure 1. Levels of GADD45 and c-myc proteins in logarithmically growing A549 cells. (*a*) Western blots showing the effects of drugs on GADD45 α, β and γ and c-myc expression. Cells were treated for 24 h with different marine-derivative agents at their respective IC_{50} evaluated after 72 h. Picture is representative of one experiment repeated three times with similar results. (*b*) The histograms report the densitometric analysis from three experiments performed as in (*a*). (*c*) RT-PCR showing the effects of drugs on c-myc mRNA expression. Cells are treated as in (*a*). M: molecular weight marker (ΦX 174 *Hae*III digest). Picture shows one experiment performed in duplicate.

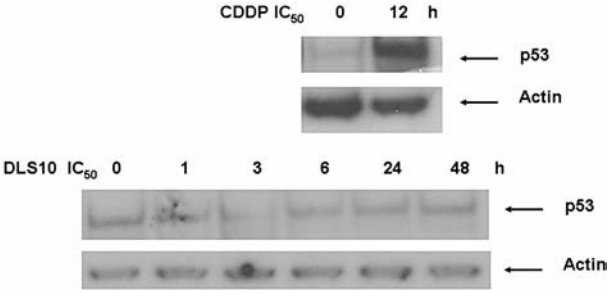

Figure 2. Effects of DLS10 on p53 protein level. Western blots showing the effects of DLS10 on p53 protein level. Cisplatin (CDDP) was the positive controls. A549 cells were treated with DLS10 for different times. Figures are representative of three replicate experiments yielding similar results.

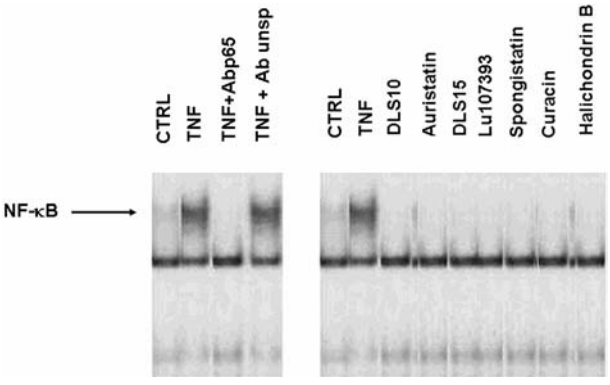

Figure 3. Gel EMSA of NF-κB complexes. Nucleic extracts of A549 cells, which were treated with different drugs for 24 h (as in Fig. 1a), were incubated with labeled probe containing a NF-κB site and with designed antibodies for 30 min. The position of NF-κB complex is shown at the left. CTRL: untreated cells, TNF 1000 U/ml for 24 h is the positive standard, Ab-p65 and Ab unspecific are positive and negative control for NF-κB translocation. Picture is one representative of three independent experiments.

after drug exposure (Fig. 2). Moreover, basal levels of p53 were observed after treatment with all marine derived compounds (data not shown), suggesting that p53 is likely not involved in the observed G_2-M arrest and GADD45 modulation induced by these drugs.

Apoptosis-induction. Since NF-κB is activated by most chemotherapeutic agents like VCR and vinblastine, two well-known inhibitors of microtubule assembly [14], we analyzed NF-κB nuclear translocation by electrophoretic mobility shift assay (EMSA) in nuclear protein extracts of treated or untreated cells (Fig. 3). TNF was used to confirm NF-κB translocation: p65 antibodies (against the p65 subunit of NF-κB) inhibited translocation, whereas unspecific antibodies did not. Interestingly, none of the marine-derived agents induced NF-κB translocation to the nucleus after 24 h of treatment (Fig. 3).

DNA secondary fragmentation (apoptosis-related) was measured by FBA in time-dependence studies. For all

compounds, apoptosis started 24 h after treatment with the IC_{50} and increased up to 72 h (Fig. 4). Necrotic effects were excluded since the percentage of DNA present in the loading fraction (LF) was less than 20%, suggesting that no fragmented DNA was present in this frac-

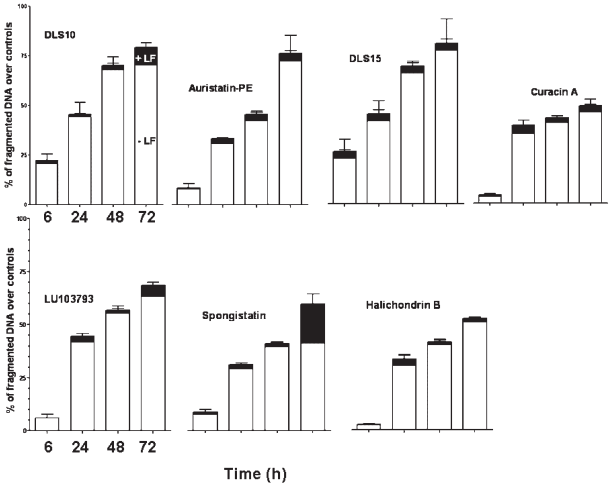

Figure 4. Determination of apoptosis by FBA. The kinetics of induction of DNA secondary fragmentation (apoptosis-related) in A549 cells was evaluated by FBA. Cells were incubated for different times with different agents at their IC_{50}. Data are expressed as mean ± SE of three independent experiments performed at least in duplicate. The black portion of the histogram represent the % of fragmented DNA already present before loading on filter (LF: loading fraction).

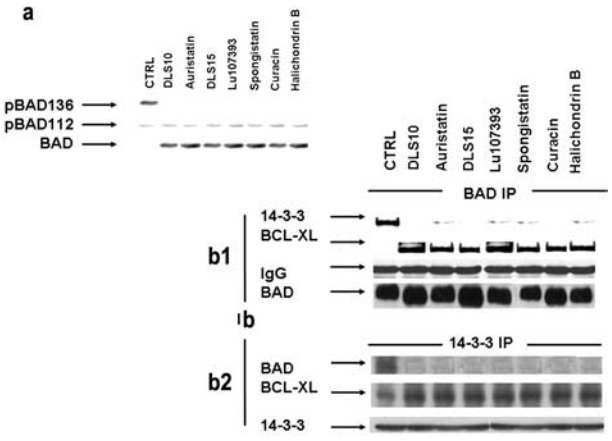

Figure 5. BAD phosphorylation status and formation of BAD containing complexes after treatment with marine derived agents. (*a*) A549 cells were treated with different drugs for 24 h and processed for Western blot analysis. Membranes were probed with antibodies directed against polyclonal phospho-specific BAD serine[112] and BAD serire[136] or with an antibody that recognizes Bad, regardless of its phosphorylation state. (*b*) Treatment of A549 cells with different drugs for 24 h resulted in the dissociation of BAD from 14-3-3 followed by binding to Bcl-XL. A phosphorylation state-independent BAD antibody (*b1*) or 14-3-3 antibody (*b2*) was cross-linked to protein G-Sepharose beads and used for IP. (*b1*) Cell lysates were incubated with the immobilized BAD antibody. Immunoblotting was used to analyze 14-3-3 and Bcl-XL bound to BAD. IgG bands are shown to confirm quality of antibody loading. (*b2*) Cell lysates were incubated with the immobilized 14-3-3 antibody. Immunoblotting was used to analyze BAD and Bcl-XL bound to 14-3-3. Figures are representative of three replicate experiments yielding similar results. CTRL: untreated cells.

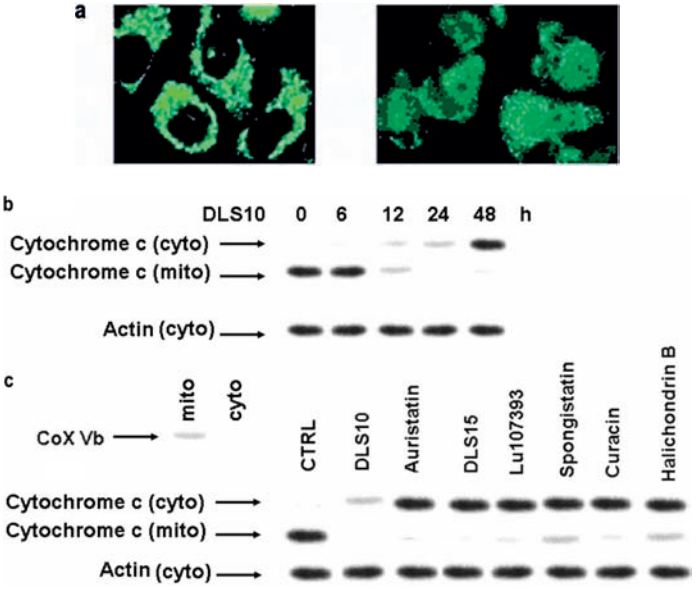

Figure 6. Cytochrome *c* release in A549 cells. (*a*) A549 cells were treated with DLS10 at the IC_{50} for 24 h and then subjected to immunofluorescence staining of cytochrome *c* to observe its release from mitochondria. (*b*) Cells were treated with DLS10 at the IC_{50} for different times. Cytosolic (cyto) or mitochondrial (mito) extracts were obtained as described under Materials and methods. To control for equal protein loading or contamination of cytosolic extracts with mitochondria, the immunoblots were stripped and reprobed with anti-actin or anti-cytochrome *c* oxidase antibodies (COX Vb). Actin is present in the cytosolic fraction, while cytochrome *c*-oxidase (COX Vb) is found in the mitochondrial (mito) but not in the cytosolic (cyto) extracts. (*c*) After treatment with different agents at the IC_{50} for 24 h, cytochrome *c* was found in the cytosolic fraction, but almost disappeared from the mitochondrial fraction. Figures are representative of three replicate experiments yielding similar results. CTRL: untreated cells.

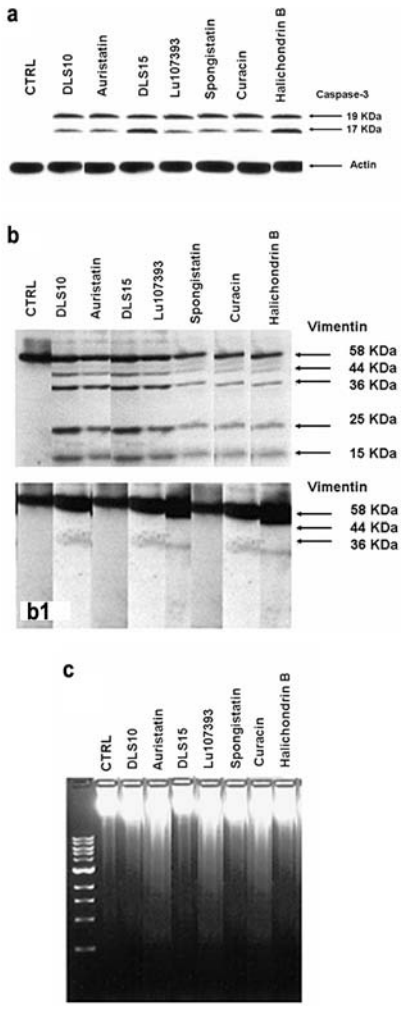

Figure 7. Caspase-3 and vimentin cleavage induced by marine-derived agents. Cells were treated for 24 h as in Fig. 1a, then harvested and lysed for Western blot analysis as described in Materials and methods. (*a*) Caspase-3 and (*b*) vimentin cleavage products after treatment with marine-derived agents are indicated by arrows. (*b1*) The cleavage of vimentin was inhibited by Z-VAD-fmk. Cells were preincubated for 0.30 h with Z-VAD-fmk and then treated for another 24 h with marine-derived agents before Western blot analysis. (*c*) Inhibition of apoptosis was evaluated by internucleosomal DNA fragmentation (gel ladder). Figures are representative of three replicate experiments yielding similar results. CTRL: untreated cells.

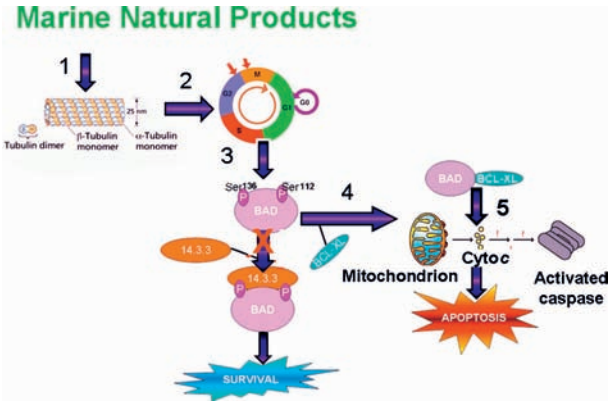

Figure 8. Schematic representation of the cascade induced by marine-derived agents. (1) Interaction with tubulin that affects microtubule assembly. (2) Cell cycle arrest at the G_2-M phase. (3) Phosphorylation of BAD, dissociation of BAD from 14-3-3 and association of BAD with BCL-XL, inhibition of survival. (4) BAD translocation to mitochondria, inactivation of BCL-XL, release of cytochrome c, activation of caspase(s) and induction of apoptosis (see Discussion).

tion. Gel laddering confirmed the generation of DNA fragmentation related to induction of apoptosis (data not shown).

We evaluated the ability of marine-derived agents to trigger phosphorylation of Bad at serine^{112} (pBAD^{112}) or at serine^{136} (pBAD^{136}). pBAD^{112} was unaffected by treatment (Fig. 5a). In contrast, each marine-derived agent inhibited the phosphorylation of Bad at serine^{136} and, consequently, increased the level of total Bad (Fig. 5a). Dephosphorylation of BAD, as reported by Masters et al. [21], results in its dissociation from the 14-3-3-complex and the subsequent binding to Bcl-XL. Co-immunoprecipitation experiments, carried out on untreated cells, showed that 14-3-3, but not Bcl-XL, co-immunoprecipitated with BAD (Fig. 5b1, lane CTRL). In contrast, after treatment, BAD dissociates from 14-3-3 and binds to Bcl-XL (Fig. 5b1). At this point BAD can move to mitochondria. Mitochondria-localized Bad promotes cell death by neutralizing the anti-apoptotic actions of Bcl-XL [31–33]. As a consequence of BAD translocation, cytochrome *c* is released to the cytoplasm, caspases are activated and finally apoptosis is triggered [31–33].

We investigated this cascade of events in A549. All marine-derived agents caused cytochrome *c* release to the cytoplasm after 24 h of treatment (Fig. 6c). For DLS10, a time course study was performed: cytochrome *c* started to appear in cytoplasm after 12 h and increased until 48 h. Simultaneously, it disappeared in the mitochondrial fraction (Fig. 6a, b). All agents induced caspase-3 cleavage, as demonstrated by the presence of the 17- and 19-kD cleavage products (Fig. 7a). Furthermore, since vimentin is an apoptotic substrate of caspase-3 during apoptosis [34, 35], its possible cleavage was analyzed. Figure 8b showed that vimentin cleavage was evident after 24 h of treatment, which induced at least four major cleavage products of 44, 36, 25 and 15 kDa. The addition of the caspase inhibitor z-DEVD-fmk, at a concentration of 10 μM, efficiently inhibited the formation of these cleavage products (Fig. 7b1) as well as the induction of apoptosis (Fig. 7c).

These data indicate that the induction of apoptosis induced by marine-derived agents is related to dephosphorylation of BAD and consequential activation of mitochondrial apoptosis pathway.

Discussion

In this study the effects of different marine-derived agents, Dolastatin10, Dolastatin15, their synthetic derivatives Auristatin-PE and LU103793, Spongistatin-1, Curacin A and Halichondrin B, were studied in NSCLC A549 cells. We have shown that marine derivatives up-regulated the expression of GADD45α and γ, and induced G_2-M arrest. These effects might be mediated by suppression of c-Myc mRNA and protein expression, whose relative mRNA and protein basal levels are moderately high in A549, cells (see [36] and our data). In addition, we analyzed NF-κB nuclear translocation by EMSA in nuclear protein extracts of treated or untreated cells. Interestingly, none of the marine-derived agents induced NF-κB translocation to the nucleus. It is known that c-Myc is under the control of NF-κB and has a protective role against the apoptotic effect of cellular insults [37]. NF-κB modulates the expression of many genes that control cell survival [37]. While some of the target genes products are protective and others death inducing, the primary role of NF-κB is to promote cell survival as massive apoptosis of liver cells is observed in embryonic NF-κB-knockout mice [37]. These contradictory effects of NF-κB are probably cell type-specific and/or dependent on the inducing signal (*i.e.* the cell- and drug-specific networks). Nevertheless, in general, the activation of NF-κB increases resistance to apoptosis ordinarily induced by chemotherapy or radiation therapy [37]. Recently, Zerbini et al. [38, 39] have demonstrated that NF-κB-mediated cell-survival mechanisms in cancer cells are absolutely dependent on two GADD45 family members, GADD45 α and γ. These authors showed that down-regulation of GADD45 α and γ protein expression, presumably through induction of c-Myc, is an essential step in NF-κB-dependent escape from programmed cell death.

Our observations are rather interesting since it has been observed that in response to cellular insults by chemotherapeutic drugs such as cis-platin, 5-FU, paclitaxel, γ-ionizing radiation, and H_2O_2, c-Myc is induced and NF-κB activated [37]. In contrast, these marine derivatives do not induce c-Myc expression and NF-κB translocations. Moreover, these compounds did not induce p53. Thus, the induction of apoptosis was investigated.

The mitochondrial 'intrinsic' pathway and the transmembrane 'extrinsic' pathway are the two principal pathways leading to apoptosis, both of which converge on caspases, a family of cysteine proteases [12, 13]. Most chemotherapeutic drugs induce mitochondrial membrane permeabilization and consequent apoptosis. Permeabilization of the outer mitochondrial membrane induces the leakage of pro-apoptotic molecules including cytochrome *c*, Smac/DIABLO, HtrA2/Omi, apoptosis inducing factor and endonuclease G from the mitochondrial intermembrane space [13]. Normally apoptosis is under the control of the Bcl-2 proteins family [12, 13]. BAD is a member of the BH3-only subfamily of the Bcl-2 apoptosis-regulating proteins, which is regulated extensively by phosphorylation on serine [15, 16]. In the absence of phosphorylation, BAD are found localized to the mitochondria bound to Bcl-2 and Bcl-XL, where it can induce cell death [15, 16]. When serine^{112} and serine^{136} of BAD becomes phosphorylated, BAD is found in the cytosol, bound to 14-3-3 proteins rather than to Bcl-2 or Bcl-XL [15, 16]. This form of BAD does not promote apoptosis. It has been shown that the serine^{136} epitope of BAD represents its primary 14-3-3 binding site [15]. Thus, phosphorylation of serine^{136} and 14-3-3 binding serves as a potent inhibitory mechanism to prevent BAD-induced apoptosis. By exerting control over multiple pro-apoptotic proteins, 14-3-3 may function as a general promoter of cell survival [18]. We have found that after treatment with marine-derived agents there is a rapid dephosphorylation of BAD and its release from the complex BAD/14-3-3. At this point BAD may dimerize with Bcl-XL and translocates from cytoplasm to mitochondria, causing cytochrome *c* release in the cytoplasm with subsequent caspase 3 activation. This cascade may trigger apoptosis in A549 cells, as outlined in Figure 8. It is important to note that the NCI-ACDS study [36] reported a strong negative correlation between basal protein and mRNA levels of BCL-XL and drug sensitivity, suggesting that BCL-XL may play a unique role in general resistance to cytotoxic agents (70 000 drugs considered).

In conclusion these agents are characterized as having unique mechanisms of action and pharmacological properties. They represent potential candidates for the treatment of malignant disease, either to be used as single agents, or as part of a combination regimen. DLS10 entered in phase I clinical trials in 1990s and progressed to phase II trials. Although DLS10 is well tolerated clinically, with hematological toxicity being the main side effect, in recent phase II clinical trials, as a single agent, it lacked significant activity [40–45]. In a small phase II study (19 patients) in advanced untreated NCSLC (stage IIIB/IV) [46], DLS10, as a single agent, failed to show activity. The activity of Auristatin-PE (*Soblidotin*, *TZT-1027*) is now under study in a phase II trials in anthracycline-refractory soft tissue sarcoma [47]. A recent phase I study of intravenous TZT-1027, in combination with carboplatin, in patients with advanced solid tumors supports the development of a phase II study [48].

At least two phase II studies conducted with LU103793 do not support the further evaluation of LU103793 in metastatic breast cancer [49] and in advanced non-small-cell lung cancer [50].

Until now, no clinical studies are ongoing for Curacin A and Spongistatin (July 2006, www.ncbi.nlm.nih.gov). Among these compounds halichondrins exhibit a unique constellation of effects on the conformation of tubulin

as indicated by their effects on tubulin alkylation, on the chemical cross-linking of tubulin, and on the binding to tubulin of the hydrophobic probe, bis-8-anilinonaphthalene sulfate [10]. Such data have led to the idea that the Halichondrins interact with tubulin in a manner distinct from that of other microtubule-targeted drugs and, thus, that they might possess unique antitumor activities [10]. Because of their phenomenal biological activity in killing cancer cells (data generated in the NCI drug evaluation program) and great structural complexity, drugs were generated by chemical synthesis from Halichondrin B that led to the discovery of E7389, which is in phase I and II clinical trials [51] The ongoing phase II trial shows encouraging results (partial responses, mild to moderate side effects) [52].

In summary, the marine world has become an important source of anticancer agents with novel mechanisms of action. The continuation of preclinical and clinical studies is required to assess the exact role of this new class of compound in the treatment of patients with cancer. Marine-derived agents such as DLS10, Auristatin-PE, DLS15, LU103793, Spongistatin-1, Curacin A and Halichondrin B seem more potent than classical antitumor agents (*i.e.* CDDP) and may be considered important anticancer leads that may have development potential.

1 Newman, D. J. and Cragg, G. M. (2004) Advanced preclinical and clinical trials of natural products and related compounds from marine sources. Curr. Med. Chem. 11, 1693–1713.
2 Mayer, A. M. and Gustafson, K. R. (2004) Marine pharmacology in 2001–2: antitumour and cytotoxic compounds. Eur. J. Cancer 40, 2676–2704.
3 Newman, D. J. and Cragg, G. M. (2004) Marine natural products and related compounds in clinical and advanced preclinical trials. J. Nat. Prod. 67, 1216–1238.
4 Amador, M. L., Jimeno, J., Paz-Ares, L., Cortes-Funes, H. and Hidalgo, M. (2003) Progress in the development and acquisition of anticancer agents from marine sources. Ann. Oncol. 14, 1607–1615.
5 Garcia-Carbonero, R., Supko, J. G., Manola, J., Seiden, M. V., Harmon, D., Ryan, D. P., Quigley, M. T., Merriam, P., Canniff, J., Goss, G., Matulonis, U., Maki, R. G., Lopez, T., Puchalski, T. A., Sancho, M. A., Gomez, J., Guzman, C., Jimeno, J. and Demetri, G. D. (2004) Phase II and pharmacokinetic study of ecteinascidin 743 in patients with progressive sarcomas of soft tissues refractory to chemotherapy. J. Clin. Oncol. 22, 1480–1490.
6 Nagle, D. G., Zhou, Y. D., Mora, F. D., Mohammed, K. A. and Kim, Y. P. (2004) Mechanism targeted discovery of antitumor marine natural products. Curr. Med. Chem. 11, 1725–1756.
7 Rawat, D. S., Joshi M, C., Joshi P and Atheaya, H. (2006) Marine peptides and related compounds in clinical trial. Anticancer Agents Med. Chem. 6, 33–40.
8 Bai, R., Taylor, G. F., Schmidt, J. M., Williams, M. D., Kepler, J. A., Pettit, G. R. and Hamel, E. (1995) Interaction of dolastatin 10 with tubulin: induction of aggregation and binding and dissociation reactions. Mol. Pharmacol. 47, 965–976.
9 Cruz-Monserrate, Z., Mullaney, J. T., Harran, P. G., Pettit, G. R. and Hamel, E. (2003) Dolastatin 15 binds in the vinca domain of tubulin as demonstrated by Hummel-Dreyer chromatography. Eur. J. Biochem. 270, 3822–3828.
10 Jordan, M. A., Kamath, K., Manna, T., Okouneva, T., Miller, H. P., Davis, C., Littlefield, B. A. and Wilson, L. (2005) The primary antimitotic mechanism of action of the synthetic halichondrin E7389 is suppression of microtubule growth. Mol. Cancer. Ther. 4, 1086–1095.
11 Chang, Z., Sitachitta, N., Rossi, J. V., Roberts, M. A., Flatt, P. M., Jia, J., Sherman, D. H. and Gerwick, W. H. (2004) Biosynthetic pathway and gene cluster analysis of curacin A, an antitubulin natural product from the tropical marine cyanobacterium *Lyngbya majuscula*. J. Nat. Prod. 67, 1356–1367.
12 Wipf, P., Reeves, J. T. and Day, B. W. (2004) Chemistry and biology of curacin, A. Curr. Pharm. Des. 10, 1417–1437.
13 Verdier-Pinard, P., Sitachitta, N., Rossi, J. V., Sackett, D. L., Gerwick, W. H. and Hamel, E. (1999) Biosynthesis of radiolabeled curacin A and its rapid and apparently irreversible binding to the colchicine site of tubulin. Arch. Biochem. Biophys. 370, 51–58.
14 Hamel, E. (2003) Evaluation of antimitotic agents by quantitative comparisons of their effects on the polymerization of purified tubulin. Cell. Biochem. Biophys. 38, 1–22.
15 Ali, M. A., Rosati, R., Pettit, G. R. and Kalemkerian, G. P. (1998) Dolastatin 15 induces apoptosis and BCL-2 phosphorylation in small cell lung cancer cell lines. Anticancer Res. 18, 1021–1026.
16 Kuznetsov, G., Towle, M. J., Cheng, H., Kawamura, T., TenDyke, K., Liu, D., Kishi, Y., Yu, M. J. and Littlefield, B. A. (2004) Induction of morphological and biochemical apoptosis following prolonged mitotic blockage by halichondrin B macrocyclic ketone analog E7389. Cancer Res. 64, 5760–5766.
17 Li, Y., Singh, B., Ali, N. and Sarkar, F. H. (1999) Induction of growth inhibition and apoptosis in pancreatic cancer cells by auristatin-PE and gemcitabine. Int. J. Mol. Med. 3, 647–653.
18 Kalemkerian, G. P., Ou, X., Adil, M. R., Adil, M. R., Rosati, R., Khoulani, M. M., Madan, S. K. and Pettit, G. R. (1999) Activity of dolastatin 10 against small-cell lung cancer *in vitro* and *in vivo*: induction of apoptosis and bcl-2 modification. Cancer Chemother. Pharmacol. 43, 507–515.
19 Korsmeyer, S. J. (1999) BCL-2 gene family and the regulation of programmed cell death. Cancer Res. 59, 1693–1700.
20 Ravagnan, L., Roumier, T. and Kroemer, G. (2002) Mitochondria, the killer organelles and their weapons. J. Cell Physiol. 192, 131–137.
21 Masters, S. C., Yang, H., Datta, S. R., Greenberg, M. E. and Fu, H. (2001) 14-3-3 inhibits Bad-induced cell death through interaction with serine-136. Mol. Pharmacol. 60, 1325–1331.
22 Debernardis, D., Sire, E. G., De Feudis, P. et al. (1997) p53 status does not affect sensitivity of human ovarian cancer cell lines to paclitaxel. Cancer Res. 57, 870–874.
23 Chou, T. C. and Talalay, P. (1977) A simple generalized equation for the analysis of multiple inhibitions of Michaelis-Menten kinetic systems. J. Biol. Chem. 252, 6438–6442.
24 Chou, T. C. and Talalay, P. (1981) Generalized equations for the analysis of inhibitors of Michaelis-Menten and higher order kinetic systems with two or more mutually exclusive and nonexclusive inhibitors. Eur. J. Biochem. 115, 207–216.
25 Bertrand, R., Sarang, M., Jenkin, J., Kerrigan, D. and Pommier, Y. (1991) Differential induction of secondary DNA fragmentation by topoisomerase II inhibitors in human tumor cell lines with amplified c-myc expression. Cancer Res. 51, 6280–6285.
26 Trombino, S., Cesario, A., Margaritora, S., Granone, P., Motta, G., Falugi, C. and Russo, P. (2004) Alpha7-nicotinic acetylcholine receptors affect growth regulation of human mesothelioma cells: role of mitogen-activated protein kinase pathway (erratum in Cancer Res. 64, 1559). Cancer Res. 64, 135–145.
27 Vikhanskaya, F., Falugi, C., Valente, P. and Russo, P. (2002) Human papillomavirus type 16 E6-enhanced susceptibility to apoptosis induced by TNF in A2780 human ovarian cancer cell line. Int. J. Cancer 97, 732–739.
28 Jin, S., Tong, T., Fan, W., Fan, F., Antinore, M. J., Zhu, X., Mazzacurati, L., Li, X., Petrik, K. L., Rajasekaran, B., Wu, M. and Zhan, Q. (2002) GADD45-induced cell cycle G2-M arrest as-

sociates with altered subcellular distribution of cyclin B1 and is independent of p38 kinase activity. Oncogene 21, 8696–8704.
29 Barsyte-Lovejoy, D., Mao, D. Y. and Penn, L. Z. (2004) c-Myc represses the proximal promoters of GADD45a and GADD153 by a post-RNA polymerase II recruitment mechanism. Oncogene 23, 3481–3486.
30 Zhang, H. Y., Gu, Y. Y., Li, Z. G., Jia, Y. H., Yuan, L., An, G. S., Ni, J. H. and Jia, H. T. (2004) Exposure of human lung cancer cells to 8-chloro-adenosine induces G2/M arrest and mitotic catastrophe. Neoplasia 6, 802–812.
31 Scheid, M. P., Schubert, K. M. and Duronio, V. (1999) Regulation of bad phosphorylation and association with Bcl-x (L) by the MAPK/Erk kinase. J. Biol. Chem. 274, 31108–31113.
32 Datta, S. R., Katsov, A., Hu, L., Petros, A., Fesik, S. W., Yaffe, M. B. and Greenberg, M. E. (2000) 14-3-3 proteins and survival kinases cooperate to inactivate BAD by BH3 domain phosphorylation. Mol. Cell 6, 41–51.
33 Dougherty, M. K. and Morrison, D. K. (2004) Unlocking the code of 14-3-3. J. Cell Sci. 17, 1875–1884.
34 Byun, Y., Chen, F., Chang, R., Trivedi, M., Green, K. J. and Cryns, V. L. (2001) Caspase cleavage of vimentin disrupts intermediate filaments and promotes apoptosis. Cell Death Differ. 8, 443–450.
35 Prasad, S. C., Thraves, P. J., Kuettel, M. R., Srinivasarao, G. Y., Dritschilo, A. and Soldatenkov, V. A. (1988) Apoptosis-associated proteolysis of vimentin in human prostate epithelial tumor cells. Biochem. Biophys. Res. Commun. 249, 332–338.
36 Amundson, S. A., Myers, T. G., Scudiero, D., Kitada, S., Reed JC. And Fornace, A. J. Jr. (2000) An informatics approach identifying markers of chemosensitivity in human cancer cell lines. Cancer Res. 60, 6101–6110.
37 Pommier, Y., Sordet, O., Antony, S., Hayward, R. L. and Kohn, K. W. (2004) Apoptosis defects and chemotherapy resistance: molecular interaction maps and networks. Oncogene 2, 2934–2949.
38 Zerbini, L. F., Wang. Y, Czibere, A., Correa, R. G., Cho, J. Y., Ijiri, K., Wei, W., Joseph, M., Gu, X., Grall, F., Goldring, M. B., Zhou, J. R and Libermann, T. A. (2004) NF-kappa B-mediated repression of growth arrest- and DNA-damage-inducible proteins 45alpha and gamma is essential for cancer cell survival. Proc. Natl. Acad. Sci. USA 101, 15271.
39 Zerbini, L. F. and Libermann, T. A. (2005) Life and death in cancer. GADD45 alpha and gamma are critical regulators of NF-kappaB mediated escape from programmed cell death. Cell cycle 4, 18–20.
40 Kindler, H. L., Tothy. PK., Wolff, R., McCormack, R. A., Abbruzzese, J. L., Mani, S., WadeOliver, K. T. and Vokes, E. E. (2005) Phase II trials of dolastatin-10 in advanced pancreaticobiliary cancers. Invest. New Drugs 235, 489–493.
41 Perez, E. A., Hillman, D. W., Fishkin, P. A., Krook, J. E., Tan, W. W., Kuriakose, P. A., Alberts, S. R. and Dakhil, S. R. (2005) Phase II trial of dolastatin-10 in patients with advanced breast cancer. Invest. New Drugs 23, 257–261.
42 Hoffman, M. A., Blessing, J. A. and Lentz, S. S. (2003) Gynecologic Oncology Group Study. A phase II trial of dolastatin-10 in recurrent platinum-sensitive ovarian carcinoma: a Gynecologic Oncology Group study. Gynecol Oncol. 89, 95–98.
43 Saad, E. D., Kraut, E. H., Hoff, P. M., Moore, D. F. Jr., Jones, D., Pazdur, R. and Abbruzzese, J. L. (2002) Phase II study of dolastatin-10 as first-line treatment for advanced colorectal cancer. Am. J. Clin. Oncol. 25, 451–453.
44 Margolin, K., Longmate, J., Synold, T. W., Gandara, D. R., Weber, J., Gonzalez, R., Johansen, M. J., Newman, R., Baratta, T. and Doroshow, J. H. (2001) Dolastatin-10 in metastatic melanoma: a phase II and pharmokinetic trial of the California Cancer Consortium. Invest. New Drugs 19, 335–345.
45 Vaishampayan, U., Glode, M., Du, W., Kraft, A., Hudes, G., Wright, J. and Hussain, M. (2000) Phase II study of dolastatin-10 in patients with hormone-refractory metastatic prostate adenocarcinoma (erratum in: Clin. Cancer Res 6, 4967). Clin. Cancer. Res. 6, 4205–4208.
46 Krug, L. M., Miller, V. A., Kalemkerian, G. P., Kraut, M. J., Ng, K. K., Heelan RT., Pizzo, B. A., Perez, W., McClean, N. and Kris, M. G. (2000) Phase II study of dolastatin-10 in patients with advanced non-small-cell lung cancer. Ann. Oncol. 11, 227–228.
47 de Jonge, M. J., van der Gaast, A., Planting, A. S., van Doorn, L., Lems, A., Boot, I., Wanders, J., Satomi, M. and Verweij, J. (2005) Phase I and pharmacokinetic study of the dolastatin 10 analogue TZT-1027, given on days 1 and 8 of a 3-week cycle in patients with advanced solid tumors. Clin. Cancer Res. 11, 3806–3813.
48 Greystoke, A., Blagden, S., Thomas, A. L., Scott, E., Attard, G., Molife, R., Vidal, L., Pacey, S., Sarkar, D., Jenner, A., De-Bono, J. S. and Steward, W. (2006) A phase I study of intravenous TZT-1027 administered on day 1 and day 8 of a three-weekly cycle in combination with carboplatin given on day 1 alone in patients with advanced solid tumours. Ann. Oncol. 17, 1313–1319.
49 Kerbrat, P., Dieras, V., Pavlidis, N., Ravaud, A., Wanders, J. and Fumoleau, P. EORTC (2003) Early Clinical Studies Group/ New Drug Development Office. Phase II study of LU 103793 (dolastatin analogue) in patients with metastatic breast cancer. Eur. J. Cancer. 39, 317–320.
50 Marks, R. S., Graham, D. L., Sloan, J. A., Hillman, S., Fishkoff, S., Krook, J. E., Okuno, S. H., Mailliard, J. A., Fitch, T. R. and Addo, F. (2003) A phase II study of the dolastatin 15 analogue LU 103793 in the treatment of advanced non-small-cell lung cancer. Am. J. Clin. Oncol. 26, 336–337.
51 Jordan, M. A., Kamath, K., Manna, T., Okouneva, T., Miller, H. P., Davis, C., Littlefield, B. A. and Wilson, L. (2005) The primary antimitotic mechanism of action of the synthetic halichondrin E7389 is suppression of microtubule growth. Mol. Cancer Ther. 4, 1086–1095.
52 O'Hanlon, L. H. (2006) Scientists are searching the seas for cancer drugs. J. Natl. Cancer. Inst. 98, 662–663.